A FUNDAMENTAL STUDY ON DEVELOPMENT OF RAPID WATER PERMEABILITY TEST FOR NEAR-SURFACE LAYER OF CONCRETE

(Translation from Proceedings of JSCE, No.627/V-44, August 1999)

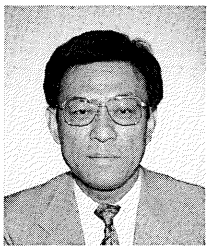
Masami SHOYA

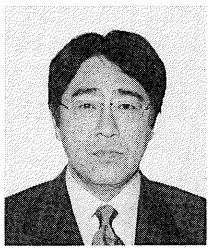
Yoichi TSUKINAGA


Mikio SASAKI

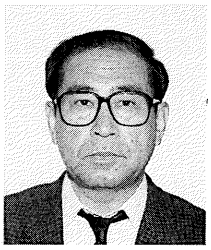
Shuichi SUGITA

The applicability of a new in-situ test method for the permeability of concrete surface layers, the original concept for which was proposed by the authors as a water-pressure in rubber tube method, is examined. In order to clarity the basic concept of this "rapid water permeability test", water permeation from the test hole is described using a basic equation of pressure diffusion. The effects of factors relating to water permeation are summarized using the diffusivity estimated from this basic diffusion equation, and the mutual relationship between estimated diffusivity and that obtained in conventional indoor water permeability tests is examined. In conclusion, this method is judged promising for in-situ testing for the assessment of water permeability and as a simplified indoor test of the diffusivity of the surface layer of concrete.

Key Words : *permeability, in-situ test, rubber tube, water pressure, rapid water permeability coefficient, water penetration, diffusion theory*

Masami Shoya is a professor in the Department of Civil Engineering at Hachinohe Institute of Technology. He received his Dr. Eng. from Hokkaido University in 1984 and has written many papers on concrete durability and shrinkage.

Yoichi Tsukinaga is a professor in the Department of Architectural Engineering at Hachinohe Institute of Technology, Hachinohe, JAPAN. He received his Dr. Eng. from Nihon University in 1998 and has been engaged in research work on the durability of concrete structures and non-destructive testing.

Mikio Sasaki is a professor in the Department of Civil Engineering at Hachinohe Institute of Technology. He received his Dr. Eng. from Hokkaido University in 1978 and his studies have centered on the problems of hydraulic engineering, coastal engineering, and river engineering.

Shuichi Sugita is a professor in the Department of Civil Engineering at Hachinohe Institute of Technology. He received his Dr. Eng. from Hokkaido University in 1996 and has been engaged in research work on cementitious materials for concrete.

---

1. INTRODUCTION

Concrete is an essentially porous material which contains several types of void and also exhibits defects such as cracks caused during placement by external forces, and by environmental conditions, etc. These voids and cracks increase the permeability of concrete and are the primary factors limiting the durability of a concrete structure. In particular, the function of the surface layers of concrete is to protect against penetration and diffusion of external deterioration factors such as oxygen, carbon dioxide, chloride ions, moisture, and so on. That is, assessing the mechanism or degree of penetration and diffusion of external deterioration factors through the surface layers of concrete can give valuable information useful for quality control, construction management, maintenance, and deterioration diagnosis.

Permeability can be assessed by a water permeability test if the deterioration factor is a liquid. However, a relatively large-scale set-up is needed to apply high pressure to the concrete and then measure either the amount of water that penetrates into the concrete or the water's penetration depth. It is usually carried out as a laboratory test. Demand for various kinds of structure management and deterioration diagnosis means that a simple method of carrying out water permeability tests needs to be established.

Simple water permeability tests that allow pressure to be applied on site have been proposed: GWT (Germann's water permeation test)[1] and AUTOCLAM (Clam water permeability test)[2]. In Japan, a method by Ohgishi[3] is applicable only to small sections such as walls and floors and a method by the authors[4), 5), 6)] have been proposed. The equipment used for GWT is attached firmly to the concrete surface using epoxy resin and anchor bolts, and a variable pressure up to 0.6 MPa can be applied by forcing a lid of the pressure room. In the case of AUTOCLAM, the equipment is directly attached to the concrete surface using either epoxy resin or anchor bolts, and 0.15 MPa of pressure can be applied by piston action. With the Ohgishi method, steel discs are fixed to the inside and outside of the section to be tested using bolts after piercing the wall or floor with a hole, and 2.45 MPa pressure is applied using a nitrogen gas container. As for the authors' test method, equipment fitted with a rubber tube is attached to the concrete surface with epoxy resin and 0.29 MPa pressure is applied by pressurizing the water-filled rubber tube. The values obtained are the volumetric amount of water forced into concrete in the case of the GWT and Ohgishi's methods, and the fall in water pressure with the AUTOCLAM and the authors' methods. Any rapid and convenient test method for use on site requires equipment able to apply water pressure for the required time. Devices to fix the equipment to the concrete surface and to prevent leakage of pressurized water are also necessary.

In this study, the surface layer of concrete is defined as a depth up to 30-40 mm, the minimum value of cover in concrete structures. The availability of the rapid permeability test was examined as the test method to assess the water permeability of concrete up to the depth of 35 mm on the site. This development cause from observations of resin pouring into cracked concrete using a rubber tube.
In this study, it is clarified that water permeation from a test hole on the concrete surface can be expressed in terms of the pressure diffusion equation so as to obtain an understanding of the basic concept of this permeability test. The influences of various factors on water permeability[4), 5), 6)] are also summarized in terms of diffusivity estimated by considering the pressure variation in the test hole, and the relationship between the diffusivity obtained using the authors' test and that by a conventional indoor water permeability test by input method is also described. From these results, it is concluded that the coefficient of rapid water permeability, as defined in this test method, is applicable as an index of water permeability.

2. BASIC CONCEPT OF RAPID WATER PERMEABILITY TEST

2.1 Equipment used and test method

Figure 1 is a schematic diagram of the test equipment. It includes a neoprene rubber tube 15 mm in diameter connected to a pressure gauge. The tube is 50 mm long and has a wall thickness of 3 mm. A coupler is used to attach the rubber tube to the concrete surface and the pressure pump. The main part of the equipment weighs about 700 g. The physical and mechanical properties of the rubber used are given in Table 1.

In the experiment, a test hole 10 mm in diameter and 35 mm in depth is drilled into the concrete. After removing the concrete debris from the test hole using a wire brush and compressed air, the coupler plug is bonded to the

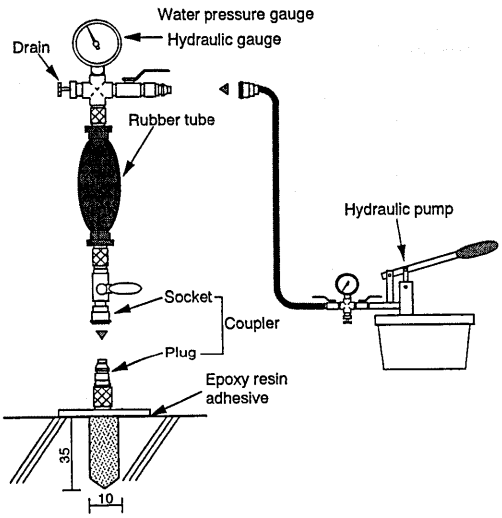

Fig.1 Schematic diagram of rapid water permeability test

Table 1 Properties of rubber used in rapid test

Hardness (Hs : JIS A)	Tensile strength (MPa)	Elongation (%)	Permanent set *1 (%)
47	25.5	550	13

Tests conducted in accordance with JIS K 6301
*1 : Maintain 22 ℃ ×500 hours

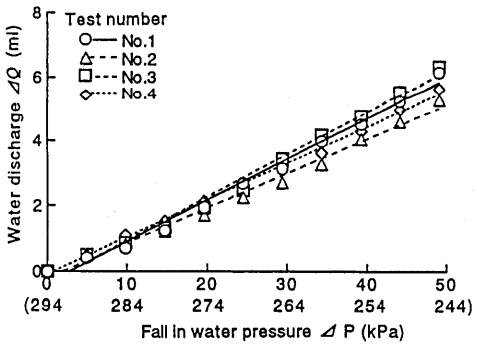

Fig. 2 Fall in water pressure ΔP versus water discharge ΔQ

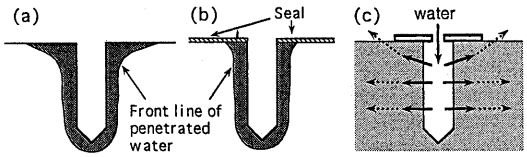

Fig.3 Schematic diagram of water penetration (a), (b) and flow of water (c)

concrete surface with an epoxy resin adhesive. Water is forced into the rubber tube using a pressure pump, and all air bubbles are removed through the drain. The pressure is maintained at about 314 kPa. The test hole and the plug are filled with water through an injection needle inserted to the bottom of the test hole, and a rubber tube with pressure gauge is connected to the test hole with the coupler. The initial pressure is adjusted to 294 kPa using the drain and the tap at the socket is opened to allow water permeation. The fall in pressure ΔP and elapsed time T are measured, and coefficient a and exponent b are calculated using equation (1).

$$\Delta P = a\, T^{b} \qquad (1)$$

where ΔP : fall in water pressure (kPa)
T : elapsed time (sec)

Figure 2 shows the relation between the fall in water pressure ΔP and the water discharge ΔQ when the water pressure is reduced in steps of 5 kPa by allowing water to escape from the drain, starting from the initial pressure of 294kPa. It can be assumed that the amount of water discharged from the drain ΔQ is the amount of water that has penetrated the concrete. The relation between the fall in water pressure ΔP and the water discharge ΔQ is confirmed to be almost linear within the range of water pressures from 294 kPa to about 245 kPa. Consequently, the water pressure fall ΔP is a convenient parameter that can be used instead of the amount of penetrated water.

As shown in Table 4 and Fig.13, there exists little influence of the spacing of test hole at the concrete surface or the distance to the edge of concrete on the test value, if the spacing or the distance is equal to or greater than 75 mm. In addition, as shown in Fig.3, if the test surface is not sealed, water also flow out into the direction of the open air from the test hole due to pressure loading. The closer the concrete surface, the greater the penetration depth of water, the measured value of the coefficient of rapid water permeability, and its coefficient of variation. Therefore, in this study, the test hole spacing or the distance to the edge from a test hole was made 75 mm and the test surface was sealed for an area of 75 mm radius.

2.2 Theoretical consideration of permeability

a) Basic equation

A large number of theoretical studies in which the water permeability of concrete is treated as a one-dimensional phenomenon have been published, including a paper by Murata[7] in 1961. However, few theoretical studies have treated the phenomenon as a two-dimensional or three-dimensional problem. In this test method, if water flow in the depth direction is ignored, it is possible to treat the diffusion of water two-dimensionally as it spreads in concentric circles from the test hole. Based on this understanding, the diffusion of water can be hypothesized as a two-dimensional plane problem. Thus, referring to Murata's study, a basic equation is introduced.

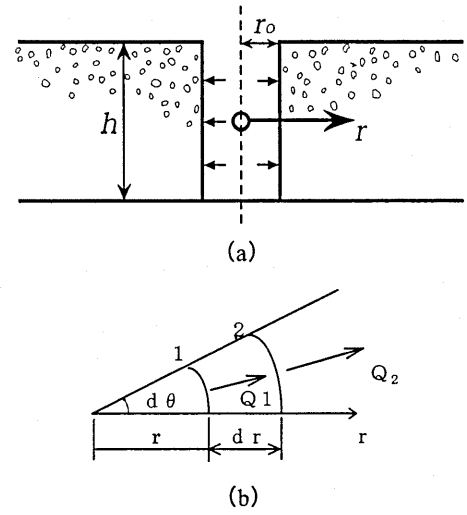

Fig. 4 (a) Definition of symbols and (b) water flow in concrete

Water migrates into the concrete from the pressurized test hole. Consider a case where the water migrates at velocity u. As shown in Fig.4, polar coordinates are set up in the sample with height h. Area 1 is defined at the distance $r \geqq r_0$ from the origin and area 2 is defined by the slightly greater distance r+dr from area 1. The amount of water Q_1 which flows into the area between areas 1 and 2 in time increment dt is given by equation (2).

$$Q_1 = u(r)hd\theta r dt \tag{2}$$

The amount of water Q_2 which flows outward from area 2 toward in time increment dt is given by the following equation:

$$Q_2 = (u + \frac{\partial u}{\partial r}dr)hd\theta(r+dr)dt \tag{3}$$

Then, the increment in permeated water ΔQ between areas 1 and 2 is obtained by the following equation:

$$\Delta Q = Q_1 - Q_2 = u\,h\,d\,\theta r dt - \{(u + \frac{\partial u}{\partial r}dr)hd\theta(r+dr)dt\} \tag{4}$$

Increment ΔQ can be obtained by the following equation if high order infinitesimals are omitted:

$$\Delta Q = -\frac{\partial(r\,u)}{\partial r}dr\,A\frac{dt}{r} \tag{5}$$

where $A = r\,d\theta h$

Velocity u falls in the positive direction of r. Therefore, this increment ΔQ develops due to elastic deformation of the infinitesimal element dr and ΔQ is equal to the volume contraction of this part. This compression phenomenon develops because the pressure p increases by only dp in time dt between areas 1 and 2 being permeated.

If it is assumed that the elastic modulus of water and concrete are common, dp can be written as the following equation:

$$dp = E\frac{\Delta Q}{A\,dr} \tag{6}$$

On the other hand, the temporal change in pressure dp is given by the following equation:

$$dp = \frac{\partial p}{\partial t} dt \tag{7}$$

Equation (8) is then obtained by substituting equations (5) and (7) into equation (6), assuming that the flow of water in concrete follows Darcy's law.

$$\frac{\partial p}{\partial t} = -E\left(\frac{u}{r} + \frac{\partial u}{\partial r}\right) \tag{8}$$

Therefore, u is given by the following equation, in which the coefficient of permeability is k and the density of water is w_0:

$$u = -\frac{k}{w_0}\frac{\partial p}{\partial r} \tag{9}$$

The following two-dimensional equation (10) is then obtained from equations (8) and (9):

$$\frac{\partial p}{\partial t} = \beta^2\left(\frac{\partial^2 p}{\partial r^2} + \frac{1}{r}\frac{\partial p}{\partial r}\right) \tag{10}$$

where $\beta^2 = \dfrac{kE}{w_0}$ (11)

Equation (10) shows that the phenomenon of water permeability in concrete results in a pressure distribution. It also shows that the parameter which dominates permeability is diffusivity β^2 only.

b) Solution of basic equation

Water in the hollowed part is at pressure p_0, where p_0 is a time-dependent value and can be represented as $p_0 = F(t)$. The initial condition and the boundary condition in this case can be described by equations (12), (13), and (14) below, and the pressure distribution p can be solved as shown in equation (15). The efferent process is shown in the appendix. Incidentally, $F(t)$ represents the pressure p_0 in the hollow part, as above-mentioned, but $F(t)$ also equals $F(0) - \alpha\sqrt{t}$ because p_0 can be written as a function of $\sqrt{t}$, according to equation (19) shown later. Here, $F(0)$ is the pressure in $t=0$ (294 kPa in this study).

initial conditions

$$p(r, 0) = 0 \qquad r_0 > 0, \quad t = 0 \tag{12}$$

boundary conditions

$$p(r_0, t) = p_0(t) \qquad r = r_0 \tag{13}$$

$$p(\infty, t) = 0 \qquad r \to \infty \tag{14}$$

$$p = F(0)\frac{1}{\displaystyle\int_0^{\infty}\frac{e^{-u^2}}{2\beta\sqrt{tu}+r_0}du}\int_0^{\frac{r-r_0}{2\beta\sqrt{t}}}\frac{e^{-u^2}}{2\beta\sqrt{tu}+r_0}du + \int_0^1\frac{\partial F}{\partial\tau}\frac{1}{\displaystyle\int_0^{\infty}\frac{e^{-u^2}}{2\beta\sqrt{t(1-\tau)}u+r_0}du} \times \int_{\frac{r-r_0}{2\beta\sqrt{t(1-\tau)}}}^{\infty}\frac{e^{-u^2}}{2\beta\sqrt{t(1-\tau)}u+r_0}du\,d\tau \tag{15}$$

In the experiment, the water penetration depth $Dm(= r - r_0)$ is measured by splitting the specimen after a fixed time t. Then, diffusivity β^2 is calculated by iteration assuming a pressure p at position Dm is 98 kPa[7]. A

Table 2 Chemical composition and physical properties of cement

Type of cement	Chemical composition (%)			Specific gravity	Blaine's specific surface area (cm^2/g)	Setting time (hr : min)		Compressive strength of 40 mm cubes (MPa)		
	MgO	SO_3	Ig. loss			Initial set	Final set	3 day	7 day	28 day
Ordinary (OPC)	2.2	2.1	1.0	3.16	3,330	2 : 18	3 : 28	16.2	25.2	41.8
High early-strength (HPC)	1.4	3.1	1.1	3.15	4,560	1 : 53	3 : 03	28.7	37.8	48.8
Moderate heat (MPC)	1.7	1.8	0.7	3.20	3,170	3 : 10	4 : 20	10.8	15.8	35.7
Blast-furnace slag (BC)	3.9	1.8	1.0	3.05	3,790	3 : 10	4 : 25	12.4	22.7	43.5

Table 3 Proportions of concrete mixtures

W/C (%)	Type of cement	G max (mm)	Slump (cm)	Air (%)	s/a (%)	Unit weight (kg/m^3) W	S	S	G	AE agent (C×wt%)	HWR *1
55	OPC	5	(187) *2	5.5	(3.1) *3	260	473	1,448	–	0.014	–
		15	8.2	5.8	47.6	176	320	858	955	0.022	–
		20	8.5	4.3	44.6	168	305	819	1,029	0.026	–
		25	9.0	4.5	42.6	160	291	798	1,086	0.033	–
		40	7.3	4.2	39.6	154	280	751	1,158	0.036	–
30	OPC	20	8.5	5.0	39.6	171	570	635	980	0.049	0.99
40			9.2	4.7	41.6	171	428	718	1,019	0.032	–
55			7.8	5.6	44.6	168	305	819	1,029	0.026	–
70			7.0	4.4	47.6	168	240	901	1,003	0.023	–
55	OPC	20	8.7	5.1	44.6	168	305	819	1,029	0.026	–
	HPC		7.2	4.4	44.0	171	311	802	1,032	0.031	–
	MPC		9.1	5.3	44.6	168	305	821	1,031	0.024	–
	BC		7.4	4.6	45.6	160	291	849	1,024	0.031	–

*1 : High-range water-reducing agent *2 : Flow (mm) *3 : S/C

theoretical solution to equation (15) is given in the appendix and its validity is verified by comparing with numerical analysis[8].
Incidentally, the water permeability in the one-dimensional case is given as follows by setting a new coordinate χ such that the concrete surface $(r-r_0)$ is at $\chi = 0$.

$$p = \frac{1}{f_1}\int_0^t F(\tau)\frac{x}{4\beta\tau^{3/2}}e^{-\frac{x^2}{4\beta^2\tau}}d\tau \tag{16}$$

where $$f_1 = \int_0^\infty e^{-u^2}du = \frac{\sqrt{\pi}}{2} \tag{17}$$

A comparison of the two-dimensional and one-dimensional solutions is shown in a figure (App. Fig. 3). The difference between the results is too large for water permeation to be approximated by a one-dimensional solution in this case.

3. OUTLINE OF EXPERIMENT

3.1 Materials and mixture proportions

Four types of Portland cement were used, as shown in Table 2. The coarse aggregate used was crushed hard

sandstone with a density of 2.71 g/ml, and five types with a maximum size ranging from 5 mm to 40 mm were used. The fine aggregate was pit sand with a fineness modulus of 2.76 and a density of 2.68 g/ml. A chemical air-entraining admixture was added; this consists essentially of natural resin acid salt. Further, in the case of the mixture with a water-cement ratio of 30 %, a high-range water-reducing agent containing a high-condensation aromatic sulfonic acid compound was also used.

To carry out the rapid water permeability tests, the attachment was bonded to the concrete surface with epoxy resin, which had a viscosity of 2×10^5 cps at 20 °C, a tensile strength of 27.5 MPa (JIS K 6911) and a hardening time of 6 hours at 20 °C.

The mix proportions of concrete were chosen to investigate the influence of maximum aggregate size, water-cement ratio, and type of cement, and they are shown in Table 3. In tests to investigate the influence of age, coefficient of water content, and temperature, ordinary Portland cement and the coarse aggregate with a maximum size of 20 mm were used, and the mix proportion with a water-cement ratio of 55%, a target slump of 8 cm, and a target air entrainment of 5% was selected. In the test to investigate the influence of specimen diameter, mortar specimens with a water-cement ratio of 55% and an air content of 5% were used.

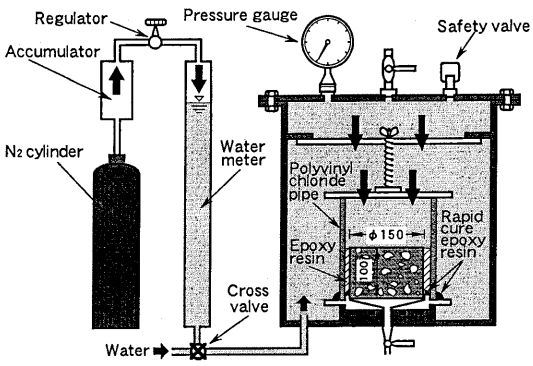

Fig. 5 Schematic diagram of water permeability test by input method

3.2 Specimens

The specimens used for the rapid water permeability test were cylinders measuring ϕ 150×150 mm. The specimens for indoor water permeability tests by the input method were cylinders measuring ϕ 150×100 mm. Each test was carried out on six specimens in the case of the rapid water permeability tests, and on three for the indoor water permeability tests. However, some measured results were abnormal in the rapid water permeability test, because leakage of a small amount of water sometimes occurred from joints in the equipment or at the bond interface. Therefore, in this test, nine specimens were actually prepared and six data were extracted by taking into account the emergence of abnormal values.

As for the test surface, the influence of bleeding was taken into consideration by choosing the bottom of the specimens as the test surface in both the rapid water permeability test and the indoor water permeability test. The specimens were made according to JIS A 1132 and compaction was by thrusting with a tamping rod.

3.3 Curing method

The specimens were cured in water for 28 days and then continuously dried for 7 days in the laboratory at 20 °C and 60 % RH[7]. They were then supplied for the tests.

3.4 Indoor water permeability test by input method[7]

A schematic diagram of the water permeability test by the input method is shown in Fig.5. The input method entails applying a water pressure of 981 kPa for 48 hours. After the test, the specimens were split open and the depth of water penetration measured. The diffusivity was then calculated by the following equation:

$$\beta^2 = \alpha \frac{Dm^2}{4t\xi^2} \tag{18}$$

where β^2 : diffusivity by input method
α : coefficient related to pressurization time
Dm : depth of water penetration
t : time required
ξ : coefficient related to water pressure

4. TEST RESULTS AND DISCUSSION

4.1 Time-dependent characteristics of water permeation and definition of coefficient of rapid water permeability

Figure 6 shows the relation between elapsed time t and the fall in water pressure ΔP for different water-cement ratios after 24 hours of permeation by water. The relationship closely resembles power equation (1).

Figure 7 shows the relation between elapsed time t and coefficient a and exponent b, as evaluated from equation (1) using all measured data up to time t. Coefficient a increases with elapsed time and is also higher with greater water-cement ratios. Exponent b changes depending on the water-cement ratio in the early stages of measurement. However, exponent b has a value close to 0.5 when the elapsed time reaches about 7,200 seconds (2 hours) independent of the water-cement ratio. In this power equation, both constants a and b must be determined, and the procedure lacks in the simplicity of the evaluation. With coefficient b fixed at 0.5, equation (1) can be re-written as equation (19) and coefficient a alone can be regarded as the index of water permeability.

Figure 8 shows the relation between the square root of time $\sqrt{t}$ and the fall in water pressure ΔP up to 7,200 seconds. As shown in equation (19), ΔP can be expressed as a function of $\sqrt{t}$.

In this test, it was decided to take measurements for 2 hours (7,200 seconds), and coefficient a was newly defined and denoted as the coefficient of rapid water permeability. Various investigations were then carried using this coefficient a. Incidentally, in the Clam water permeability test proposed by Basheer[2], the water permeation is regressed with the square root of elapsed time and the coefficient of permeability is defined as the gradient of the regression line. The method of definition is exactly the same as in the authors' test method.

4.2 Influence of various factors on coefficient of rapid water permeability[5), 6)]

Table 4 shows a list of the results for tests on age, water-cement ratio, type of cement, maximum size of aggregate, diameter of specimen (i.e. the test hole spacing or distance of test hole from edge), coefficient of water content, and temperature, respectively. The coefficient of rapid water permeability a, coefficient of variation V, depth of water penetration Dm, diffusivities (as obtained by solving the diffusion equation for two-dimensional or one-dimentional water permeability; they

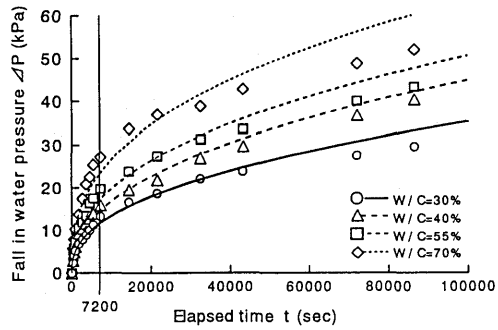

Fig.6 Elapsed time t versus fall in water pressure ΔP

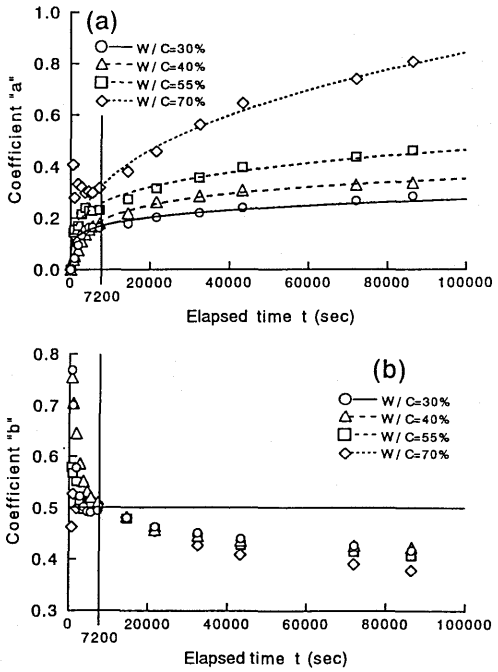

Fig.7 Elapsed time t versus coefficient "a" or "b"

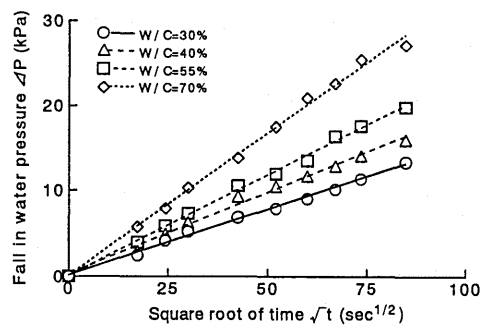

Fig.8 Square root of elapsed time $\sqrt{t}$ versus fall in water pressure ΔP

Table 4 Results of rapid tests and indoor tests

Test items		Coefficient of rapid water permeability a (kPa/s$^{1/2}$)	Coefficient of variation V (%)	Depth of penetration of water Dm (mm)	Diffusivity by two-dimensional solution β_{II}^2 ($\times 10^{-8}$ m^2/s)	Diffusivity by one-dimensional solution β_{I}^2 ($\times 10^{-8}$ m^2/s)	Diffusivity by input method β^2 ($\times 10^{-8}$ m^2/s)
Age +7 : drying period (day)	3+7	0.716	30.3	29.2	85.20	7.97	98.07
	7+7	0.412	21.9	16.1	10.30	2.17	29.40
	28+7	0.226	23.6	12.9	4.80	1.31	6.91
	91+7	0.147	18.5	7.7	1.15	0.46	1.43
Water-to-cement ratio (%)	30	0.157	20.5	10.8	2.82	0.90	1.19
	40	0.186	26.9	12.4	4.20	1.20	6.80
	55	0.226	23.6	12.9	4.80	1.31	6.91
	70	0.324	29.3	13.8	6.20	1.55	11.17
Type of cement	OPC	0.235	23.1	12.4	4.30	1.22	9.12
	HPC	0.118	20.7	8.2	1.38	0.53	5.36
	MPC	0.265	29.2	18.4	13.20	2.70	10.08
	BC	0.216	27.5	10.1	2.45	0.80	6.04
Maximum size of coarse aggregate (mm)	5	0.207	22.7	7.2	1.06	0.43	
	15	0.278	24.4	9.2	2.21	0.72	
	20	0.223	28.8	15.4	7.75	1.10	
	25	0.256	23.9	14.0	7.42	2.02	
	40	0.386	41.5	14.8	8.63	1.38	
Diameter of specimen (mm)	50	0.289	39.9	15.2	9.50	1.86	
	100	0.237	29.4	13.8	7.31	1.51	
	150	0.187	25.7	13.6	5.29	1.44	
	200	0.216	24.5	12.7	4.55	1.30	
Coefficient of water content (%)	27.7	1.040	38.6	28.7	152.0	8.90	
	44.2	0.804	39.3	27.5	81.7	7.33	
	60.0	0.481	30.6	14.0	7.31	1.68	
	75.0	0.343	32.7	13.9	6.38	1.58	
	97.5	0.235	36.5	13.2	5.12	1.38	
Temperature of test (°C)	5	0.137		19.3			
	20	0.127		12.9			
	35	0.333		8.2			

are tentatively denoted as diffusivity by two-dimensional solution β_{II}^2 and diffusivity by one-dimensional solution β_{I}^2), and the diffusivity by input method β^2 (obtained from the indoor water permeability test) are shown in the table.

The authors' results obtained so far with respect to the influence of various factors[5), 6)] are summarized as follows:

a) The coefficient of rapid water permeability a reflects changes in the permeability of concrete according to age, water-cement ratio, and the type of cement, and it tends to decrease as a dense structure forms in the concrete.

b) The coefficient of rapid water permeability a increases if the diameter of the specimen is below 150 mm, and so is influenced by test hole spacing and distance to concrete edge.

c) The coefficient of rapid water permeability a increases when the maximum size of the aggregate is increased.

d) The coefficient of rapid water permeability a changes little when the coefficient of water content exceeds 60 to 70 %. However, the influence of the coefficient of water content is great and an investigation of how to correct for its effects will be necessary before applying this method to actual concrete structures.

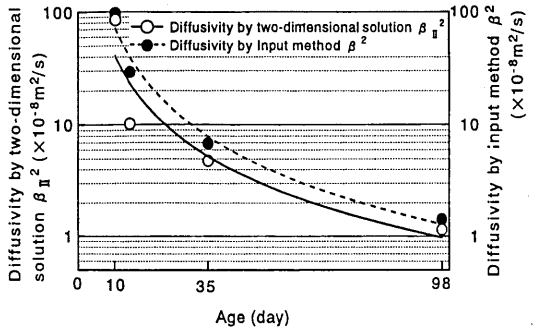

Fig.9 Age versus diffusivity by two-dimensional solution β_{II}^2 and diffusivity by input method β^2

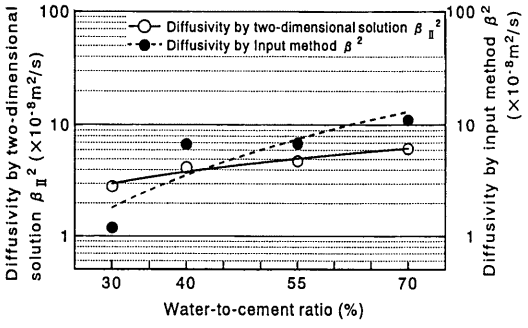

Fig.10 Water-to-cement ratio versus diffusivity by two-dimensional solution β_{II}^2 and diffusivity by input method β^2

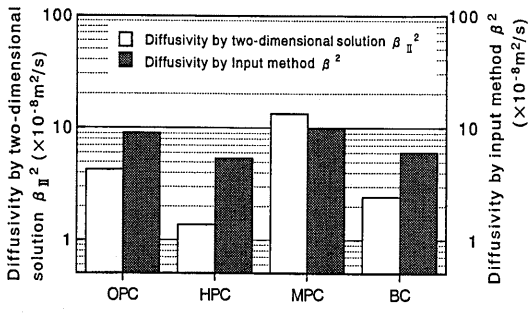

Fig.11 Type of cement versus diffusivity by two-dimensional solution β_{II}^2 and diffusivity by input method β^2

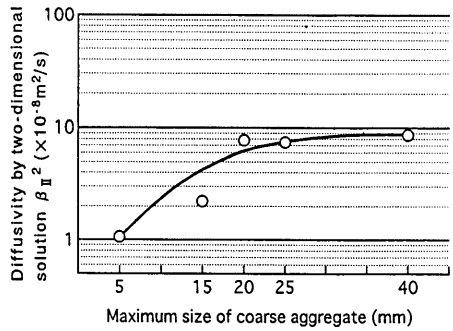

Fig.12 Maximum size of coarse aggregate versus diffusivity by two-dimensional solution β_{II}^2

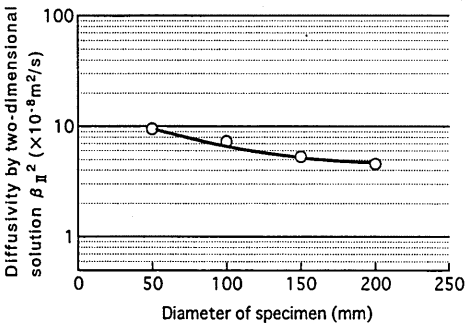

Fig.13 Diameter of specimen versus diffusivity by two-dimensional solution β_{II}^2

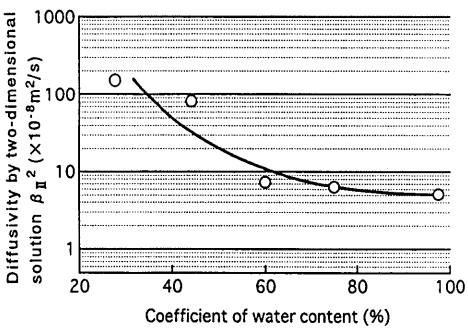

Fig.14 Coefficient of water content versus diffusivity by two-dimensional solution β_{II}^2

e) The coefficient of rapid water permeability a does not vary greatly over the range of temperatures between 5 °C and 20 °C, but a pronounced change takes place at a temperature of 35 °C, perhaps because the rubber tube itself is susceptible to large plastic deformations at higher temperatures.

f) The coefficient of variation V of the coefficient of rapid water permeability a rangs from 30 to 40 %, when the diameter of the specimen is small, the maximum aggregate size is large, the specimen is particularly dry or soaked, or the concrete is young and the water-cement ratio is relatively high. However, variation V showed an averages of 24 % if these factors are excluded.

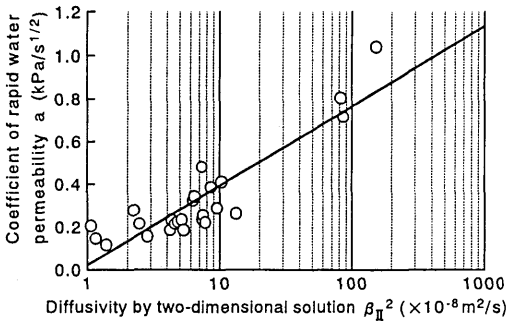

Fig.15 Diffusivity by two-dimensional solution β_{II}^2 versus coefficient of rapid water permeability a

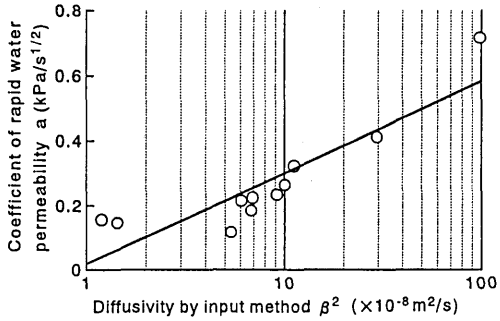

Fig.16 Diffusivity by input method β^2 versus coefficient of rapid water permeability a

4.3 Evaluation of diffusivity by two-dimensional solution

The change in diffusivity obtained by the two-dimensional solution β_{II}^2 is shown in Fig.9 to Fig.14. These figures also include the change in diffusivity β^2 by the input method. Figure 15 shows the relation between diffusivity by two-dimensional solution β_{II}^2 and the coefficient of rapid water permeability a.

The diffusivity obtained by the two-dimensional solution β_{II}^2 reflects changes in age, water-cement ratio, cement type, maximum aggregate size, and specimen diameter. It also corresponds to changes in the coefficient of rapid water permeability a. Further, the diffusivity given by the two-dimensional solution β_{II}^2 ranged from 1 to 1000×10^{-8} m^2/s, which corresponds well to the range of diffusivity β^2 obtained by Murata[7]. Therefore, the rapid water permeability test appears promising as a convenient indoor test method for assessing diffusivity.

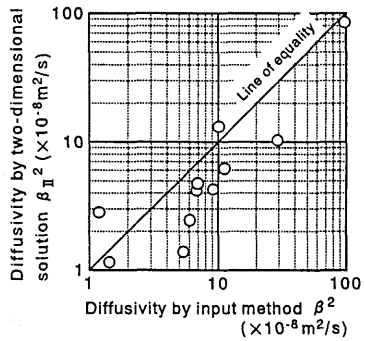

Fig. 17 Diffusivity by input method β^2 versus diffusivity by two-dimensional solution β_{II}^2

4.4 Relationship to diffusivity by input method β^2

Figure 16 shows the relation between diffusivity by input method β^2 and the coefficient of rapid water permeability a. Figure 17 shows the relation between diffusivity by input method β^2 and diffusivity by the two-dimensional solution β_{II}^2. As Fig.9 to Fig.11 show, the changes in diffusivity by input method β^2 reflect variations in concrete performance due to age, water-cement ratio, and type of cement, and also correspond well to changes in the coefficient of rapid water permeability a and diffusivity by the two-dimensional solution β_{II}^2. The diffusivity by input method β^2 is close to the value given by the two-dimensional solution β_{II}^2. These results suggest the possibility that the coefficient of rapid water permeability may be available as an index of water permeability.

5. AVAILABILITY OF RAPID WATER PERMEABILITY TEST AND FUTURE PROBLEMS TO BE SOLVED

This rapid water permeability test is based on measuring changes in pressure using the elasticity of a rubber tube. The equipment is light, with a weight of about 700 g. The test attachment of 38 mm square in equipment is bonded to the concrete surface using epoxy resin. The equipment is simple and convenient to use as compared with other methods of applying water pressure, and the simplicity of the test seems to be a major advantage.

In applying the method to an existing structure, it is possible to examine all directions and positions, including the top, bottom, and sides of a member, because of the simple way in which pressure is applied. However, the improvement of the equipment is needed because the rubber tube can not stand itself without the supporting

device.

The coefficient of variation of the coefficient of rapid water permeability a is rather large, at just less than 30 %, though this value includes the variation in water permeability of the concrete itself as well as that resulting from measurement. However, the coefficient of variation of the diffusivity obtained using Murata's input method was 24 to 30 %[7], so the precision of this test is approximately equivalent to that in the tests carried out by Murata. Figg's method for water permeability, in which a water head of 100 mm is set up, shows coefficients of variation from 32 to 40 % even when using a dried specimen of fixed mass[9]. From this perspective, the precision of this rapid test appears satisfactory.

The coefficient of rapid water permeability reflects the water permeability of the surface layer of concrete and also corresponds well to the diffusivity obtained by the two-dimensional solution and by the input method. As a result, this test is promising as an assessment of the water permeability or diffusivity of structures in-situ or indoor. However, the coefficient of rapid water permeability is strongly influenced by the water content of the concrete, and an investigation of a correction method for this coefficient is necessary for cases where high accuracy is required. The problem of water content is a common one in permeability tests of this kind, and a means of measuring water content to high precision and by a simple procedure is desired.

Further investigations will be needed, before this method can be applied to extensive concrete on the following points such as the effect of an initial pressure on the test value, that of the change of the physical quality of rubber tube under high temperature up to 35 °C, and the relation between the degree of the deterioration and the water permeability of concrete, and the development of index value showing the deterioration level.

6. CONCLUSIONS

The conclusions obtained from the investigations of the rapid water permeability test are summarized as follows:

(1) Water permeation can be expressed by diffusion theory for this test, thus clarifying the basic concept of the test method. A solution to the diffusion equation that takes the pressure changes in the test hole into account is proposed.
(2) The coefficient of rapid water permeability is obtained as the gradient of the linear relationship between the measured fall in water pressure and the square root of elapsed time up to 2 hours.
(3) The water permeability in this rapid test is influenced strongly by the water content of the concrete being measured. The coefficient of variation of the coefficient of rapid water permeability ranged from 18 to 29 % and was an average of 24 % if abnormal cases are ignored.
(4) The coefficient of rapid water permeability and diffusivity obtained by a two-dimensional method obtained from theoretical analysis corresponded to the diffusivity by the input method in indoor water permeability tests. This confirms that the rapid water permeability test is suitable as a simplified indoor test for assessing the diffusivity of the surface layer of concrete.
(5) The rapid water permeability test suffers from problems such as the temperature dependency of the rubber tube itself. However, it is also judged promising as an in-situ test for the permeability of concrete.

Acknowledgements

The authors would like to thank Dr. Hara Tadakastu of Nihon Univercity and Mr. Domon Katsuji, previously of Sho-Bond Corporation and now of Kako Construction Corporation.

Appendix

Introduce a new variable ξ defined by the following equation:

$$\xi = \frac{r - r_0}{2\beta\sqrt{t}} \qquad \text{(App.1)}$$

Each differential operator is given as

$$\left.\begin{aligned}\frac{\partial}{\partial t} &= -\frac{1}{2}\frac{\xi}{t}\frac{\partial}{\partial \xi}\\ \frac{\partial}{\partial r} &= \frac{1}{2\beta\sqrt{t}}\frac{\partial}{\partial \xi}\\ \frac{\partial^2}{\partial r^2} &= \frac{1}{4\beta^2 t}\frac{\partial^2}{\partial \xi^2}\end{aligned}\right\} \qquad \text{(App.2)}$$

Then, equation (10) is given as

$$-\frac{1}{2}\frac{\xi}{t}\frac{\partial p}{\partial \xi} = \frac{1}{4t}\left\{\frac{\partial^2}{\partial \xi^2} + \frac{1}{\xi+\zeta}\frac{\partial}{\partial \xi}\right\}p \qquad \text{(App.3)}$$

where $\zeta = \dfrac{r_0}{2\beta\sqrt{t}}$ (App.4)

Equation (App.3) is rewritten as equation (App.5).

$$\frac{\partial^2 p}{\partial \xi^2} + \left(\frac{1}{\xi+\zeta} + 2\xi\right)\frac{\partial p}{\partial \xi} = 0 \qquad \text{(App.5)}$$

Assuming the following equation:

$$\frac{\partial}{\partial \xi} = D_\xi \qquad \text{(App.6)}$$

Equation (App.5) is rearranged as follows:

$$\left\{D_{\xi\xi} + \left(\frac{1}{\xi+\zeta} + 2\xi\right)D_\xi\right\}p = 0 \qquad \text{(App.7)}$$

The following equation is obtained as the solution of equation (App.7):

$$D_\xi p = \frac{e^{-\xi^2}}{\xi+\zeta} \qquad \text{(App.8)}$$

Then, the following equation is obtained as the solution of equation (App.8):

$$p = c_1 - c_2\int_\xi^\infty \frac{e^{-u^2}}{u+\zeta}du \qquad \text{(App.9)}$$

Equation (App.9) satisfies equation (App.7). Taking for integration constants c_1 and c_2 to meet the initial conditions is equation (12) and boundary conditions is equation (13), the solution will be given.
Setting $-c_2 = c_2$ and $f(\zeta)$ into following equation:

$$f(\zeta) = \int_0^\infty \frac{e^{-u^2}}{u+\zeta}du \qquad \text{(App.10)}$$

equation (App.9) becomes

$$p = c_1 + c_2 f(\zeta)\{1 - \frac{1}{f(\zeta)} \int_0^{\xi} \frac{e^{-u^2}}{u+\zeta} du\} \quad \text{(App.11)}$$

$c_1=0$, because it is $t=0$ and $\xi \to \infty$, namely $p=0$ from the initial conditions and the boundary conditions. Therefore, the following equation results:

$$p = c_2 f(\zeta)\{1 - \frac{1}{f(\zeta)} \int_0^{\xi} \frac{e^{-u^2}}{u+\zeta} du\} \quad \text{(App.12)}$$

Next, the integration constant c_2 is assumed to meet the boundary conditions. Set $p_0=F(\lambda)=u_0$, from $r=r_0$ and $t=\lambda$. Then, the pressure in the hollow part is as follows from equation (App.12):

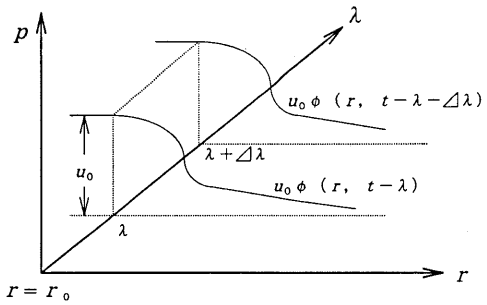

App. Fig.1 Approximation of $\Delta\lambda$

$$p = c_2 f(\zeta_\lambda)\{1 - \frac{1}{f(\zeta_\lambda)} \int_0^{\xi_\lambda} \frac{e^{-u^2}}{u+\zeta_\lambda} du\} \Big|_{\xi_\lambda = 0} = c_2 f(\zeta_\lambda) = u_0 \quad \text{(App.13)}$$

where $\zeta_\lambda = \dfrac{r_0}{2\beta\sqrt{t-\lambda}}$ $\xi_\lambda = \dfrac{r-r_0}{2\beta\sqrt{t-\lambda}}$ (App.14)

Integration constant c_2 is as follows at time λ:

$$c_2 = \frac{u_0}{f(\zeta_\lambda)} \quad \text{(App.15)}$$

Therefore, pressure p is given by the following equation:

$$p(r, t-\lambda) = u_0\{1 - \frac{1}{f(\zeta_\lambda)} \int_0^{\xi_\lambda} \frac{e^{-u^2}}{u+\zeta_\lambda} du\} \quad \text{(App.16)}$$

If ϕ is defined as follows:

$$\phi = 1 - \frac{1}{f(\zeta_\lambda)} \int_0^{\xi_\lambda} \frac{e^{-u^2}}{u+\zeta_\lambda} du \quad \text{(App.17)}$$

then pressure p is given by the following equation:

$$p(r, t-\lambda) = u_0 \phi(r, t-\lambda) \quad \text{(App.18)}$$

Equation (App.18) is satisfied with $p=0$ when $t<\lambda$ and with $p|_{r=r0}=p_0$ when $t>\lambda$. However, this gives the pressure in the hollow part only at the moment of time λ, since the pressure changes with time. Now, suppose that the pressure is approximated by equation (App.18) before and after this moment in time. That is, suppose that u_0 is approximated during the time $\Delta\lambda$. Then, equation (App.18) is not correct beyond time $\lambda + \Delta\lambda$. Therefore, as shown in App.Fig.1, the correct pressure p_s in $\lambda \sim \lambda + \Delta\lambda$ is as follows:

$$p_S = u_0\{\phi(r,t-\lambda) - \phi(r,t-\lambda-\Delta\lambda)\} = u_0[\phi(r,t-\lambda) - \{\phi(r,t-\lambda) + \frac{\partial\phi(r,t-\lambda)}{\partial\lambda}\Delta\lambda\}] = u_0\{-\frac{\partial\phi(r,t-\lambda)}{\partial\lambda}\Delta\lambda\}$$

Here, as shown below, the differentiation of t and λ is interchangeable.

$$-\frac{\partial \phi(r,t-\lambda)}{\partial \lambda}=\frac{\partial \phi(r,t-\lambda)}{\partial t} \qquad \text{(App.19)}$$

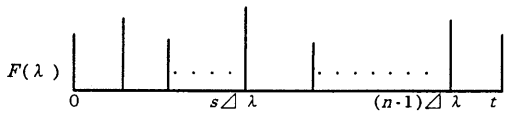

App. Fig. 2 Approximation of time sΔλ

Then, pressure p_s is as follows:

$$p_S = u_0 \frac{\partial \phi(r,t-\lambda)}{\partial t}\Delta\lambda \qquad \text{(App.20)}$$

Pressure p is represented by the following equation from App.Fig.2 because $p \mid_{r=r0} = F(\lambda)$ in $\lambda = 0 \sim \lambda$.

$$p=\sum_{s=0}^{n-1} F(s\Delta\lambda)\frac{\partial \phi}{\partial t}\Delta\lambda \qquad \text{(App.21)}$$

Then,

$$p=\lim_{\Delta\lambda\to 0}\sum_{s=0}^{n-1} F(s\Delta\lambda)\frac{\partial \phi}{\partial t}\Delta\lambda$$

The following equation (App.22) is a solution that satisfies the boundary conditions with changing pressure in the hollow part:

$$p=\int_0^t F(\lambda)\frac{\partial \phi(r,t-\lambda)}{\partial t}d\lambda \qquad \text{(App.22)}$$

Equation (App.23) is obtained by expressing equation (App.22) in r and t.

$$p=\int_0^t F(\lambda)\Bigg[\frac{\frac{r_0}{4\beta(t-\lambda)^{3/2}}\int_0^\infty \frac{e^{-u^2}}{(u+\frac{r_0}{2\beta\sqrt{t-\lambda}})^2}du}{\{\int_0^\infty \frac{e^{-u^2}}{u+\frac{r_0}{2\beta\sqrt{t-\lambda}}}du\}^2}\times\int_0^{\frac{r-r_0}{2\beta\sqrt{t-\lambda}}}\frac{e^{-u^2}}{u+\frac{r_0}{2\beta\sqrt{t-\lambda}}}du$$

$$-\int_0^{\frac{r-r_0}{2\beta\sqrt{t-\lambda}}}\frac{r_0}{4\beta(t-\lambda)^{3/2}}\frac{e^{-u^2}}{(u+\frac{r_0}{2\beta\sqrt{t-\lambda}})^2}du+\frac{1}{2}\frac{r-r_0}{2\beta(t-\lambda)^{3/2}}\frac{e^{-(\frac{r-r_0}{2\beta\sqrt{t-\lambda}})^2}}{\frac{r-r_0}{2\beta\sqrt{t-\lambda}}+\frac{r_0}{2\beta\sqrt{t-\lambda}}}\Bigg]d\lambda \qquad \text{(App.23)}$$

When the pressure $F(\lambda)$ in the hollow part changes simply, the use of the following solution for p is convenient. That is, equation (App.22) simplifies the following equation from equation (App.19):

$$p=-[F(\lambda)\phi(r,t-\lambda)]_0^t+\int_0^t \frac{\partial F(\lambda)}{\partial \lambda}\phi(t,t-\lambda)d\lambda \qquad \text{(App.24)}$$

Where ϕ in the 1st term on the right side of equation (App. 24) is as follows:

$$\phi(r,t-\lambda)\big|_{\lambda=t}=1-1=0 \qquad \text{(App.25)}$$

$$\phi(r,t-\lambda)\big|_{\lambda=0} = 1-\frac{1}{\int_0^{\infty}\frac{e^{-u^2}}{2\beta\sqrt{t}\,u+r_0}}\int_0^{\frac{r-r_0}{2\beta\sqrt{t-\lambda}}}\frac{e^{-u^2}}{2\beta\sqrt{t}\,u+r_0}du \qquad \text{(App.26)}$$

Then, equation (App.23) becomes

$$p = F(0)\{1-\frac{1}{\int_0^{\infty}\frac{e^{-u^2}}{2\beta\sqrt{t}u+r_0}du}\times\int_0^{\frac{r-r_0}{2\beta\sqrt{t-\lambda}}}\frac{e^{-u^2}}{2\beta\sqrt{t}\,u+r_0}du\}$$

$$+\int_0^{t}\frac{\partial F(\lambda)}{\partial\lambda}\{1-\frac{1}{\int_0^{\infty}\frac{e^{-u^2}}{2\beta\sqrt{t-\lambda}\,u+r_0}du}\times\int_0^{\frac{r-r_0}{2\beta\sqrt{t-\lambda}}}\frac{e^{-u^2}}{2\beta\sqrt{t-\lambda}\,u+r_0}du\}\,d\lambda \qquad \text{(App.27)}$$

Now, introduce the following variable τ to facilitate the calculation of a solution:

$$\tau=\frac{\lambda}{t} \qquad \text{(App.28)}$$

Then, ϕ can be written as follows:

$$\phi(r,t) = 1-\frac{1}{\int_0^{\infty}\frac{e^{-u^2}}{2\beta\sqrt{t}\,u+r_0}du}\int_{0}^{\frac{r-r_0}{2\beta\sqrt{t}}}\frac{e^{-u^2}}{2\beta\sqrt{t}\,u+r_0}du = \frac{1}{\int_0^{\infty}\frac{e^{-u}}{2\beta\sqrt{t}u+r_0}du}\int_{\frac{r-r_0}{2\alpha\sqrt{t}}}^{\infty}\frac{e^{-u^2}}{2\beta\sqrt{t}u+r_0}du \qquad \text{(App.29)}$$

and

$$\phi(r,t-\lambda) = 1-\frac{1}{\int_0^{\infty}\frac{e^{-u^2}}{2\beta\sqrt{t-\lambda}\,u+r_0}du}\times\int_0^{\frac{r-r_0}{2\beta\sqrt{t-\lambda}}}\frac{e^{-u^2}}{2\beta\sqrt{t-\lambda}\,u+r_0}du$$

$$= \frac{1}{\int_0^{\infty}\frac{e^{-u^2}}{2\beta\sqrt{t-\lambda}\,u+r_0}du}\times\int_{\frac{r-r_0}{2\alpha\sqrt{t-\lambda}}}^{\infty}\frac{e^{-u^2}}{2\beta\sqrt{t-\lambda}\,u+r_0}du \qquad \text{(App.30)}$$

Finally, the pressure distribution p is given by equation (15).

$$p = F(0)\frac{1}{\int_0^{\infty}\frac{e^{-u^2}du}{2\beta\sqrt{t}u+r_0}}\int_0^{\frac{r-r_0}{2\beta\sqrt{t}}}\frac{e^{-u^2}}{2\beta\sqrt{t}u+r_0}du + \int_0^{1}\frac{\partial F}{\partial\tau}\frac{1}{\int_0^{\infty}\frac{e^{-u^2}}{2\beta\sqrt{t(1-\tau)}\,u+r_0}du}$$

$$\times\int_{\frac{r-r_0}{2\beta\sqrt{t(1-\tau)}}}^{\infty}\frac{e^{-u^2}}{2\beta\sqrt{t(1-\tau)}u+r_0}du\,d\tau \qquad (15)$$

Equation (15) is a very complicated analytical solution and computation is difficult because the integrand changes

suddenly close to $\tau = 1$ and becomes a function for which integration is unfavorable. A difference solution, that is simple to compute and whose solution is easily found, is shown as follows:

$$p_i^{n+1} = p_i^n + \Delta t \beta^2 \frac{p_{i+1} - 2p_i + p_{i-1}}{(\Delta r)^2} + \Delta t \beta^2 \frac{1}{r_i} \frac{p_{i+1} - p_{i-1}}{2\Delta r} \qquad \text{(App.31)}$$

App.Fig.3 compares the solutions, and the pressure $F(\tau)$ in the hollow part is given as follows:

$$F(\tau) = (c_1 + c_2\sqrt{\tau})p_m \qquad \text{(App.32)}$$

where p_m : typical pressure in the hallow part (98 kPa)

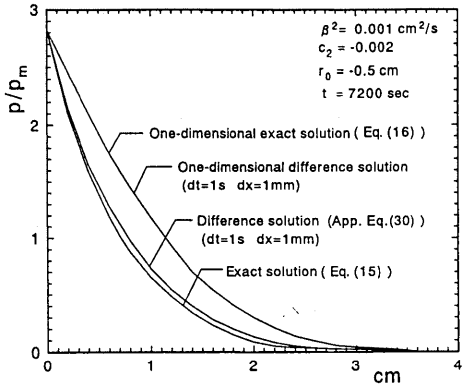

App. Fig. 3 Difference solutions and exact solutions

In App.Fig.3, $\Delta t = 1$s and $\Delta r = \Delta x = 1$mm in the differences solution. The difference solution concords with the exact solution in a one-dimensional problem when $\beta^2 = 0.0001$. In the case of the two-dimensional solution, the difference solution qualitatively with, but shows rather higher values than, the exact solution as given by equation (15). The smaller the difference, the less the variation between the difference solution and the exact solution in case of the two-dimensional problem.

References

[1] Germann Instruments: GWT-4000, Germann's water permeation test; Instruction and Maintenance Manual, Germann Instruments A/S, 4p., 1996.3.

[2] Basheer, P.A.M., Montgomery, F.R., and Long, A.E.: The autoclam permeability system for measuring the in-situ permeation properties of concrete, International Conference on NDT in Civil Engineering, The British Institute of Non-destructive Testing, Vol.1, pp.235-260, 1993.4.

[3] Ohgishi, S., Tanahashi, I., Ono, H., and Mizutani, K.: Evaluation of Durability for Concrete in Terms of Water-tightness, Proc. of JCI, Vol.8, pp.113-116, 1986.6 (in Japanese).

[4] Shoya, M., and Tsukinaga, Y.: A study on Rapid Water permeability Test for Concrete, Proc. of the 21st JUCC Congress on Cement and Concrete, pp.23-28, 1994.10 (in Japanese).

[5] Tsukinaga, Y., Shoya, M, Sugita, S., and Ishibashi, M: Assessing Permeability of Near-Surface Concrete by Rapid Testing Methods, JCA Proc. of Cement & Concrete, No.50, pp.290-295, 1996.12. (in Japanese)

[6] Tsukinaga, Y., Shoya, M., Kasai, Y., and Domon, K.: Assessing Permeability of Surface Layer of Concrete by In-Situ Tests, Journal of Structural and Construction Engineering, AIJ, No.506, pp.7-14, 1998.4 (in Japanese).

[7] Murata, J.: Studies on the Permeability of Concrete, Trans. of JSCE, No.77, pp.69-103, 1961.11 (in Japanese).

[8] Sasaki, M. Shoya, M., and Tsukunaga, Y.: Theory on Permeability of Concrete, The Bulletin of Hachinohe Institute of Technology, No.6, pp.117-124, 1997.2 (in Japanese).

[9] Dhir, R.K., Hewlett, P.C., and Chan, Y.N.: Near-surface characteristics of concrete; assessment and development of in situ-test methods, Magazine of Concrete Research, Vol.39, No.141, pp.183-195, 1987.12.